www.czasopisma.pan.pl PAN POLSKA AKADEMIA NAUK www.journals.pan.pl

A R C H I V E S O F M E T A L L U R G Y A N D M A T E R I A L S

Volume 58 2013 Issue 4

DOI: 10.2478/amm-2013-0179

S.V. SHALUPAEV*, A.N. SERDYUKOV*, G.S. MITYURICH**, M. ALEKSIEJUK***, Y.V. NIKITJUK*, A.A. SEREDA*

MODELING OF MECHANICAL INFLUENCE OF DOUBLE-BEAM LASER ON SINGLE-CRYSTALLINE SILICON

MODELOWANIE MECHANICZNEGO WPŁYWU PODWÓJNEJ WIĄZKI LASEROWEJ NA KRYSTALICZNY KRZEM

The results of finite-element modeling of controlled laser thermosplitting of crystalline silicon are presented. The case of treatment by two laser beam with wavelengths, namely 0.808 μm and 1.06 μm is studied. Calculations of the thermoelastic fields formed in a single-crystalline silicon wafer as a result of consecutive two-beam laser heating and action of coolant were performed for silicon crystalline orientations: (100), (110), (111). Modeling was performed for circular and U-shaped laser beams. The results received in the presented work, can be used for the process optimization concerning the precise separation of silicon wafers by laser cutting.

Keywords: laser cutting, thermoelastic stresses, silicon wafers, crack

W pracy przedstawiono wyniki modelowania metodą elementów skończonych termorozszczepiania krystalicznego krzemu przy pomocy wiązek laserowych. Analizowano przypadek działania dwóch wiązek laserowych o długości fali 0,808 μm i 1,06 μm. Obliczenia pól termosprężystych, formowanych w krystalicznym waflu krystalicznym, prowadzono jako efekt kolejnych działań dwuwiązkowego ogrzewania laserowego i chłodzenia dla orientacji (100), (110), (111) krystalicznego krzemu. Modelowanie prowadzone było dla wiązek o przekroju kolistym oraz w kształcie litery U. Otrzymane wyniki mogą być wykorzystane do optymalizacji precyzyjnego cięcia laserem wafli krzemowych.

1. Introduction

The single crystal materials as silicon, gallium arsenide and quartz are widely applied in modern electronic industry. The traditional technologies to treat these materials are sufficiently limited mainly concerning the presence of a defective area along the treatment line. Recently the method of controlled laser thermosplitting has been developed and has started to be used for the dimensional treatment of the above-listed crystals [1-4]. This method ensures a high-precision material division following the laser-induced crack formation and scribing. The formation of that dividing crack comes from the action of the thermoelastic stresses, which appear as a result of the consecutive laser heating of treated material and the aftercooling of heated area by a coolant [5]. The main advantages of controlled laser thermosplitting are high accuracy of division, enhanced speed of treatment, wastelessness and cleanness.

It is known [6] that the successful solution of several problems of laser technologies for the material treatment is ensured at the expense of using two-beam treatment methods based on the simultaneous action on a material two laser beams with different wavelengths. In the case of controlled laser thermosplitting of silicate glasses and alumina ceramics application of two-beam technology provides an increase in dimensional processing efficiency [7-13]. Modeling results of two-beam laser thermosplitting of silicon wafers by radiation of the YAG-laser are summarized in [14]. Nevertheless, the previous calculations of thermoelastic fields have been made without taking into account the elastic anisotropy of their crystalline structure, although various physical properties of crystalline materials can be qualitatively varied in comparison to isotropic mediums [15].

As it was shown in [16], the use of U-shaped beams at controlled laser thermosplitting of isotropic materials allows to block a deviation of the laser-induced crack towards the microdefects at the edges of a sample.

Therefore, the process modeling for two-beam controlled laser thermosplitting of the silicon (concerning the cubic crystalline system with a glance of its anisotropy), including the use of U-shaped laser beams, is very important. This modeling data are discussed in the presented paper.

2. Numerical modeling

Modeling of silicon wafers laser thermosplitting process has been made within the limits of an unbounded thermoelasticity problem in quasi-static state with the use of a finite

* DEPARTMENT OF PHYSICS "GOMEL STATE UNIVERSITY BY F. SKORINA", SOVETSKAYA 104, 246019 GOMEL, BELARUS

** EDUCATIONAL ESTABLISHMENT "BELARUSIAN TRADE AND ECONOMICS UNIVERSITY OF CONSUMER COOPERATIVES", GOMEL

*** INSTITUTE OF FUNDAMENTAL TECHNOLOGICAL REASEARCH POLISH ACADEMY OF SCIENCES, 5B PAWIŃSKIEGO, 02-106 WARSZAWA, POLAND

element method [17]. As a main criteria, which determines a sense of the laser-induced crack propagation, the criterion of the maximum tensile stresses has been used [18]. The density (ρ), specific heat (c), heat conductivity coefficient (λ) and linear thermal expansion coefficient (α) of silicon were assumed as ρ =2330 kg/m^3, c=758 Joule/(kg×K), λ =10^9 Watt/(m×K), and α =2.33·10^{-6} K^{-1} respectively [19, 20].

The calculations of the thermoelastic fields formed in a single-crystalline silicon wafer were made considering the result of consecutive laser heating and refrigerant action. It includes analysis for the six various cases: I a – section (100) at cutting in direction [001]; I b – section (100) at cutting in direction [011]; II a – section (110) at cutting in direction [1-10]; II b – section (110) at cutting in direction [001]; II c – section (110) at cutting in direction [1-11], III – section (111) at cutting in direction [1-10].

The Hooke law for the anisotropic materials can be written down in the matrix form [19, 21]:

$$\sigma_i = \sum_{k=1}^{6} C_{ik}(\varepsilon_k - \varepsilon_k^t),$$

where

$$\sigma_1 = \sigma_{xx}, \quad \sigma_2 = \sigma_{yy}, \sigma_3 = \sigma_{zz}, \quad \sigma_4 = \sigma_{yz},$$
$$\sigma_5 = \sigma_{zx}, \quad \sigma_6 = \sigma_{xy} \text{ are stresses,}$$

$$\varepsilon_1 = \varepsilon_{xx}, \quad \varepsilon_2 = \varepsilon_{yy}, \varepsilon_3 = \varepsilon_{zz}, \quad \varepsilon_4 = 2\varepsilon_{yz},$$
$$\varepsilon_5 = 2\varepsilon_{zx}, \quad \varepsilon_6 = 2\varepsilon_{xy} \text{ are elastic deformations,}$$

$$\varepsilon_1^t = \alpha_x \Delta T, \quad \varepsilon_2^t = \alpha_y \Delta T, \varepsilon_3^t = \alpha_z \Delta T,$$
$$\varepsilon_4^t = 0, \quad \varepsilon_5^t = 0, \quad \varepsilon_6^t = 0 \text{are thermal deformations.}$$

For cubic crystals the matrix $\{C_{ik}\}$is given elsewhere [22]:

Constants of elastic stiffness are used for calculations: C_{11} =1.656·10^5 MPa, C_{12} =0.6386·10^5 MPa, C_{44} =0.7953·10^5 MPa [23].

Calculations for two layouts of zones of laser and coolant influence, shown in Figures 1 and 2, have been made.

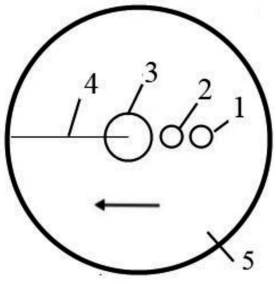

1 – laser beam with wavelength 1.06 μm;
2 – laser beam with wavelength 0.808 μm;
3 – coolant; 4 – the laser-induced microcrack;
5 – silicon wafer.

Fig. 1. The scheme of action zone of laser radiation and coolant in the treatment plane while using laser beams with a circle cross-section. (the horizontal arrow shows the direction of workpiece travel concerning the laser beams and coolant)

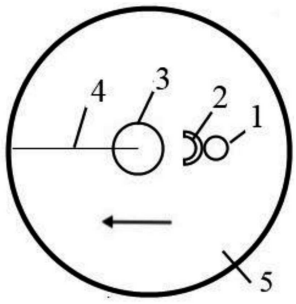

1 – laser beam with wavelength 1.06 μm;
2 – laser beam with wavelength 0.808 μm;
3 – coolant; 4 – the laser-induced microcrack;
5 – silicon wafer.

Fig. 2. The scheme of an action zone of laser radiation and coolant in the treatment plane while using circular and U-shaped beams. (the horizontal arrow shows the direction of workpiece travel concerning the laser beams and coolant)

Calculations have been made for Si-wafers with diameter Ø 31 mm under thicknesses h=0.2 mm and h=0.4 mm. Diameters of both laser beam spots in Fig. 1 and beam noted by a position 1 in Fig. 2 were D=1 mm, with their radiation power P=70 W. Internal diameter of a laser beam spot noted by a position 2 in Fig. 2 d=1 mm, external – D=1.5 mm, with radiation power P=70 W.

The velocities (v) of wafer travel towards with a laser beam and coolant was selected to be equal v=10 mm/sec and 100 mm/sec.

3. Results of modeling and their discussion

Results of calculations are presented in Tables 1-6 and in Figures 3-4. Tables 1-3 give the data of the maximum and minimum temperatures in the treated wafer for two- and one-beam action, while in Tables 4-6 calculated values of tensile and compressive stresses within the treatment zone are represented. The Fig. 3 presents the distributions of temperature fields and Fig. 4 – the fields of the thermoelastic stresses formed on the surface of single-crystalline silicon wafers of the crystalline section (111) regarding both two-beam and one-beam, with the use of a circular laser beam with wavelength 0.808 μm, schemes of controlled thermosplitting. For these calculation wafer thickness and processing speed are taken as h=200 μm and v=10 mm/sec respectively.

TABLE 1

Calculation data of the maximum and minimum temperatures of treated wafer at two-beam laser action with wavelengths 0.808 μm and 1.06 μm

Temperature of treated wafer T, K	h=200 μm		h=400 μm	
	v=10 mm/sec	v=100 mm/sec	v=10 mm/sec	v=100 mm/sec
maximum	2054	1391	1406	968
minimum	331	293	361	293

TABLE 2
Calculation data for the maximum and minimum temperatures of treated wafer at one-beam laser action with wavelengths 0.808 μm

Temperature of treated wafer T, K	h=200 μm		h=400 μm	
	v=10 mm/sec	v=100 mm/sec	v=10 mm/sec	v=100 mm/sec
maximum	1882	1293	1233	876
minimum	325	293	339	293

TABLE 3
Calculation data of the maximum and minimum temperatures of treated wafer at two-beam laser action while using the U-shaped laser beam with wavelength 0.808 μm

Temperature of treated wafer T, K	h=200 μm		h=400 μm	
	v=10 mm/sec	v=100 mm/sec	v=10 mm/sec	v=100 mm/sec
maximum	2154	1287	1467	921
minimum	334	293	363	293

As one can see from the data analysis of the maximum values of temperatures summarized in table 1 and 3, except the case of a thin plate treatment at the low speed (h=0.2 mm, v=10 mm/sec), the wafer temperature doesn't exceed the melting point of silicon. One can also notice, that the value of the silicon thermal conductivity causes a considerable decrease in maximum temperatures for the thick samples treatment in the comparison to thinner samples, when simultaneous two-beam radiation with wavelengths 0.808 μm and 1.06 μm is used. These changes reach (30-32%) comparing to the cutting plates with thickness of 200 μm and 400 μm, in the case of two-beam technology, and (32-34%) when one-beam laser treatment is applied at 0.808 μm.

One can notice that the use of the second laser beam at 1.06 μm also increases temperature maximum values within the treatment zone on 8-9% in case of wafers with thickness h=200 μm, while in case of wafers with thickness h=400 μm the increase amounts to 11-14%.

The use of U-shaped laser beam leads to appropriate change in a form of intensive heating zone. As shown further, it leads to formation of an analogous zone of compressive stresses.

Notable, that modeling of the two-beam scheme of controlled thermosplitting shown in Fig. 1 does not show big changes in the particular localization of a temperature gradient and fields of thermoelastic stresses in the comparison to one-beam analysis (see Figs 3-4).

As one can see from the data analysis summarized in Tables 4-5, the use of two-beam technology in comparing to the one-beam irradiation is increasing the value of the maximum tensile stresses in the laser treated zone. In the case of 200 μm wafer treatment the tensile stresses is increased on 13-21% while in the case of 400 μm wafer treatment on 31-37%.

Thus, the use of the two-beam technology of controlled laser thermosplitting of single-crystalline silicon with 0.808 microns and 1.06 microns irradiation becomes more effective in case of thicker samples treatment.

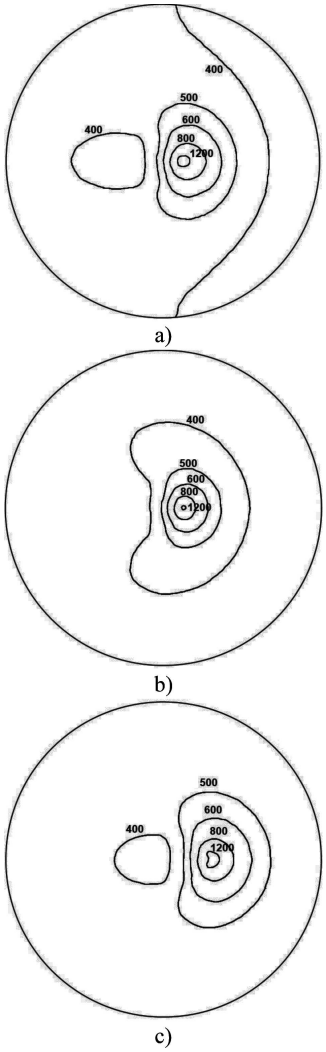

Fig. 3. Distribution of temperature fields on surfaces of silicon wafers, K:
a) – at two-beam laser action with wavelengths 0.808 μm and 1.06 μm according to the scheme shown in Fig. 1;
b) – at one-beam laser action with wavelength 0.808 μm according to the scheme shown in Fig. 1;
c) – at two-beam laser action with wavelengths 0.808 μm and 1.06 μm according to the scheme shown in Fig. 2.

The use of a U-shaped laser beam with wavelength 0.808 μm, according to the analysis of the maximum tensile and compressive stresses in the treatment zone, leads to an increase in their values in comparison to the two-beam scheme shown in Figure 1. At high speed this increase makes 2-8% for compressive stresses and 3-5% for tensile stresses, and at low speed – 15-20% and 6-10% respectively. At the same time, the power of a U-shaped beam and the power of a circular beam are equal.

The analysis of temperature stresses distribution when realizing the scheme with the use of U-shaped beam shows that zones of high compressive stresses appear on each side from a treatment line in the field of the beam action. Results of the modeling allow us to conclude that the use of the scheme shown in figure 2 at appropriate treatment parameters make it possible to block a deviation of a crack towards the microdefects at the edges of the sample.

TABLE 4

Calculated values of tensile and compressive stresses within the treatment zone at two-beam laser action with wavelengths 0.808 μm and 1.06 μm

Case	Maximum stresses in a treatment zone σ_y, MPa	h=200 μm		h=400 μm	
		v=10 mm/sec	v=100 mm/sec	v=10 mm/sec	v=100 mm/sec
I a	tensile	53.7	116	31.4	3.8
	compressive	-280	-168	-165	-95
I b	tensile	57.2	10.9	31.6	3.7
	compressive	-285	-169	-166	-95
II a	tensile	58.0	11.7	31.7	3.5
	compressive	-292	-177	-173	-100
II b	tensile	69.0	14.4	35.5	4.8
	compressive	-330	-199	-184	-106
II c	tensile	63.0	12.3	33.4	3.9
	compressive	-315	-188	-179	-103
III	tensile	63.6	12.6	34.6	4.2
	compressive	-309	-184	-181	-103

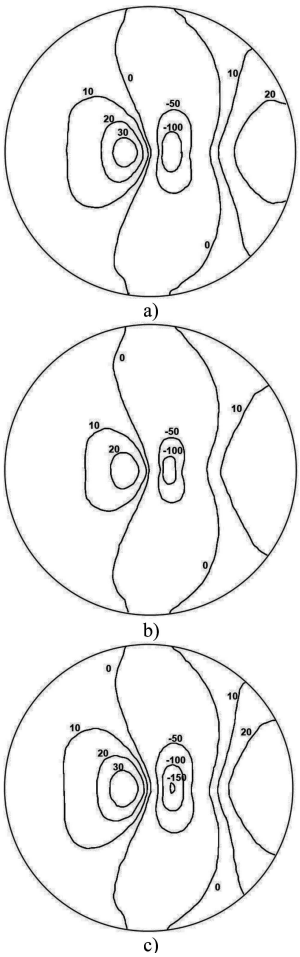

Fig. 4. Distribution of the thermoelastic stresses fields on the surface of silicon wafers, MPa:
a) – at two-beam laser action with wavelengths 0.808 μm and 1,06 μm according to the scheme shown in Fig. 1;
b) – at one-beam laser action with wavelength 0.808 μm according to the scheme shown in Fig. 1;
c) – at two-beam laser action with wavelengths 0.808 μm and 1.06 μm according to the scheme shown in Fig. 2

TABLE 5

Calculated values of tensile and compressive stresses within the treatment zone at one-beam laser action with wavelength 0.808 μm

Case	Maximum stresses in a treatment zone σ_y, MPa	h=200 μm		h=400 μm	
		v=10 mm/sec	v=100 mm/sec	v=10 mm/sec	v=100 mm/sec
I a	tensile	47.5	9.8	23.0	2.8
	compressive	-261	-156	-146	-85
I b	tensile	47.4	9.1	23.,1	2.7
	compressive	-266	-157	-147	-85
II a	tensile	48.1	9.8	23.2	2.6
	compressive	-273	-164	-153	-89
II b	tensile	57.3	12.1	26.1	3.6
	compressive	-309	-185	-163	-95
II c	tensile	52.2	10.3	24.5	2.9
	compressive	-294	-175	-158	-92
III	tensile	52.7	10.6	25.3	3.2
	compressive	-288	-171	-161	-93

TABLE 6

Calculated values of tensile and compressive stresses within the treatment zone at two-beam laser action using the U-shaped laser beam with wavelength 0.808 μm

Case	Maximum stresses in a treatment zone σ_y, MPa	h=200 μm		h=400 μm	
		v=10 mm/sec	v=100 mm/sec	v=10 mm/sec	v=100 mm/sec
I a	tensile	62.3	12.1	33.4	3.9
	compressive	-331	-170	-200	-105
I b	tensile	62.4	11.3	33,.	3.8
	compressive	-342	-173	-204	-106
II a	tensile	63.1	12.1	33.7	3.7
	compressive	-344	-178	-207	-109
II b	tensile	74.7	15.0	37.7	4.9
	compressive	-313	-202	-224	-116
II c	tensile	68.5	12.7	35.5	4.1
	compressive	-377	-192	-220	-115
III	tensile	69.2	13.2	36.8	4.4
	compressive	-368	-187	-222	-115

4. Conclusions

According to the modeling data, it was found, that for two-beam controlled laser thermosplitting of crystalline silicon (at 0.808 μm and 1.06 μm irradiation) the calculated values of tensile stresses in the treatment zone of coolant considerably exceeded the stresses formed during the one-beam treatment. Thus, the practical use of two-beam technology of controlled laser thermosplitting will provide an increase in stability of

the process aimed for the initialization and propagation of the laser-induced cracks in silicon wafers.

It is shown that application of U-shaped beam makes it possible to block a deviation of a crack towards the microdefects at the edges of the sample. Thus, the positive effect is attained at the expense of compressive stresses zone formation on each side of the laser-induced crack initialization zone.

REFERENCES

[1] A.S. Naumov, Development of division technology of instrument wafers on crystals, author's abstract of Ph.D. of Physics dissertation: 05.11.14, MSUPI, 2009.

[2] P.D. Gindin, Development of new technologies and the equipment on basis of a laser controlled thermosplitting method for treatment of instrument making parts, micro- and optoelectronics, author's abstract of Doctor of Physics dissertation: 05.11.14, MSUPI, 2009.

[3] A.N. Serdyukov, S.V. Shalupaev, Yu.V. Nikitjuk, Features of Controlled Laser Therm Cleavage of Crystalline Silicon, Crystallography Reports **55**(6), 933-937 (2010).

[4] A.N. Serdyukov, E.B. Shershnev, S.V. Shalupaev, Yu.V. Nikitjuk, V.F. Sholokh, S.I. Sokolov, Features of Controlled Laser Thermal Cleavage of Crystal Quartz, Crystallography Reports **57**(6), 792-797 (2012).

[5] V.S. Kondratenko, The method of cutting of nonmetallic materials, Patent 2024441, Russian federation, 1994.

[6] A.V. Fedin, Effect of a pulling of radiation CO_2-laser in the narrow channel at metals treatment by the combined laser radiation, Proceedings RAC. S. Physics **63**(10), 2053-2058 (1999).

[7] S.V. Shalupaev, E.B. Shershnev, Yu.V. Nikitjuk, A.A. Sereda, Two-beam laser thermal cleavage of brittle nonmetallic materials, J. Opt. Technol **73**(5), 356-359 (2006).

[8] S.V. Shalupaev, A.V. Maksimenko, V.N. Mishkovets, Yu.V. Nikitjuk, Laser cutting of ceramics materials with metallized surface, J. Opt. Technol **68**(10), 758-760 (2001).

[9] J. Junke, W. Xinbing, Cutting glass substrates with dual-laser beams, Optics and Lasers in Engineering **47**, 860-864 (2009).

[10] V.K. Sisoev, P.A. Vyatlev, A.V. Chirkov, V.A. Grozin, D.A. Konyaschenko, The concept of two-laser glass elements thermosplitting for spacecrafts, BULLETIN S.A. Lavoshkina PSUI CIA **1**, 38-44 (2011).

[11] S.V. Shalupaev, A.V. Semchenko, Yu.V. Nikityuk, Silica gel glasses after laser radiation, Material Science **21**(4), 495-501 (2003).

[12] S.V. Shalupaev, Yu.V. Nikityuk, A.A. Sereda, Laser thermal cleavage of brittle nonmetallic materials along closed curvilinear contours, J. Opt. Technol **75**(2), 75-78 (2008).

[13] S.V. Shalupaev, M. Aleksiejuk, Y.V. Nikitjuk, A.A. Sereda, A.S. Pobiyaha, Laser thermosplitting of ceramic-metal sandwich-like structures with acoustical surveillance of microcrack propagation, Archives of Metallurgy and Materials **54**(4), 963-968 (2009).

[14] J. Liu, J. Lu, X. Ni, G. Dai, L. Zhang, Y. Chen, Numerical study on thermal stress cutting of silicon wafer using two-point pulsed laser, Optica Applicata **41**(1), 247-255 (2011).

[15] A.F. Konstantinova, B.N. Grechushnikov, B.V. Bokut, E.G. Valyashko, Optical properties of crystals, Minsk, Navuka i tehnika, 1995.

[16] S.V. Shalupaev, M. Aleksiejuk, Y.V. Nikitjuk, A.A. Sereda, The analysis of laser thermosplitting of materials by using special geometry beams, Archives of Metallurgy and Materials **56**(4), 1149-1155 (2011).

[17] N.N. Shabrov, Final element method in calculations of thermal engines parts, Leningrad, Mashinostroenie, 1983.

[18] G.P. Karzov, B.Z. Margolin, V.A. Shevtsova, Physical-mechanical modeling of destruction processes, S-Petersburg, Politehnika, 1993.

[19] E.S. Falkevich, Technology of semiconductor silicon, Moscow, Metallurgiya, 1992.

[20] Yu.V. Koritskij, Reference book on electrotechnical materials, Leningrad, Energoatomizdat, 1988.

[21] T. Lackner, Determination of axisymmetric elastic constants in anisotropic silicon for a thyristor tablet, Journal of Electronic Materials **18**, 19-24 (1989).

[22] A.N. Serdyukov, S.V. Shalupaev, Yu.V. Nikityuk, A.A. Sereda, Process research of laser splitting of silicon wafers, cutout in the plane (110), Problems of physics, Mathematics and Technics **3**(12), 37-40 (2012).

[23] A.A. Blistanov, Acoustical crystals, Moscow, Nauka, 1982.

Received: 20 September 2013.